Nonlinear Fluid Slosh Coupled to the Dynamics of a Spacecraft

Lee D. Peterson*
Sandia National Laboratories, Albuquerque, New Mexico
and
Edward F. Crawley* and R. John Hansman†
Massachusetts Institute of Technology, Cambridge, Massachusetts

The dynamics of a linear spacecraft mode coupled to the nonlinear low-gravity slosh of a fluid in a cylindrical tank is investigated. Coupled, nonlinear equations of motion for the fluid-spacecraft system are derived through an assumed mode Lagrangian method. Unlike a linear model, this nonlinear model retains two fundamental slosh modes and three secondary slosh modes. An approximate perturbation solution of the equations of motion indicates that the nonlinear coupled system response involves fluid-spacecraft modal resonances not predicted by either a linear, or a nonlinear, uncoupled slosh analysis. An experiment was developed to verify and complement this analysis. Scale model fluid tanks were coupled to an electromechanical analog for the second-order oscillatory spacecraft mode. Moderate and low gravity were simulated in 1 *g* using capillary scale models, and zero gravity was simulated in parabolic flight tests on the NASA KC-135 Reduced Gravity Test Facility. The experimental results substantiated the analytical predictions. The dependence of the coupled nonlinear response on the coupled system parameters and the gravity level is illustrated and discussed.

Introduction

DURING the formulation of a spacecraft dynamic model, it is frequently assumed that the action of particular nonlinear subsystems can be accurately represented by linearized models. The slosh of a fluid mass contained within tanks aboard the spacecraft is one such subsystem. Although fluid slosh is intrinsically nonlinear, linear representations of the slosh, whether analytical or experimental, are often used to predict the resulting coupled fluid-spacecraft motion. The literature reports a variety of practical techniques for formulating such linear slosh models.[1-10]

All linear analyses share a common presumption that the slosh motion of the fluid free surface is much smaller than the dimension of the container. Therefore, a linear coupled fluid-spacecraft model will remain valid so long as either the external disturbances are small or the spacecraft and slosh natural frequencies are well separated. It may not be possible to satisfy both requirements within the constraints of a design, even with propellant management devices such as baffles and bladders. Consequently, it may be necessary to assess the linearity of the slosh model to qualify the spacecraft dynamic model.

Most experience with nonlinear slosh is limited to the response of the fluid to a prescribed motion of the container. Such *uncoupled* slosh behavior has been extensively investigated in the limit of high gravity.[11-14, 21-22] The high-gravity slosh motion generated by lateral motion of the tank will depend on the slosh wave amplitude. At intermediate amplitudes, the slosh resembles (for most fluid depths) a softening nonlinear spring: the natural frequency decreases with amplitude of the motion. At large amplitudes, more complex harmonic motion of the fluid is observed. A prescribed lateral translation of the tank no longer produces only lateral, unidirectional (planar) motion of the fluid. Transverse (nonplanar) motion of the fluid can be excited by a nonlinear coupling to the lateral fluid motion. The combination of lateral and transverse fluid motions may form simple harmonic rotary motion, multiply periodic rotary motion, and chaotic rotary motion.[14] Other analyses, which model the effects of capillarity on the fluid motion and therefore are applicable at low gravity,[15-20] do not adequately discuss the effects of capillarity on the nonlinear slosh, but complicated nonlinear motions of the fluid are possible at all gravity levels.

While a study of the uncoupled nonlinear slosh motion suggests the types of behavior that might be found in the fluid subsystem of the coupled system, it is important to realize that the uncoupled nonlinear slosh behavior may not be superposed onto a linear spacecraft structural behavior to determine the dynamics of the coupled fluid-spacecraft system. The temptation to do so is based on linear thinking. A nonlinear system embedded in a larger and otherwise linear system does not necessarily respond as simply as the nonlinear system in isolation. For this reason, it is essential that a *coupled* model be developed to predict the spacecraft motion whenever finite slosh motion is expected. Linear fluid models or even nonlinear uncoupled fluid representations will lead to a misleading prediction of coupled fluid-spacecraft dynamic behavior.

A few specific examples, available in the literature, such as Refs. 23 and 24, discuss the dynamics of a fluid-structure system in the limit of very high gravity. These studies recognized that the coupled problem is fundamentally nonlinear. However, because these previous studies considered a very specific system, many questions remain regarding the development and understanding of nonlinear coupled fluid-spacecraft models. Particularly important questions in this regard are the following:

1) For what fluid-spacecraft systems (characterized by nondimensional parameters) will a nonlinear model of the fluid be required?

2) When nonlinear coupled motion is anticipated, what is the minimum content of a fluid model that will reliably predict the coupled motion?

3) How will the nonlinear coupled motion differ from the nonlinear uncoupled motion of the fluid alone?

This paper combines analytical and experimental results from a representative study model to provide generalizable

Presented as Paper 88-2470 at the AIAA SDM Issues of the International Space Station Conference, Williamsburg, VA, April 21-22, 1988; received April 21, 1988; revision received Dec. 19, 1988.

*Member Technical Staff, Applied Mechanics Division 1524. Member AIAA.

†Associate Professor of Aeronautics and Astronautics. Member AIAA.

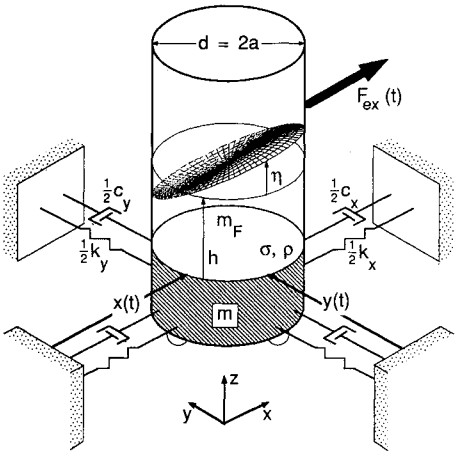

Fig. 1 Fluid-spacecraft study model investigated in this research.

answers to these questions. An analytical, nonlinear fluid model is developed by extending the work of Miles[12–14] to include a low-gravity equilibrium free surface and by generalizing the work of Limarchenko[15–20] to include vibratory spacecraft motion. Coupled, nonlinear equations of motion are found that are valid to cubic order in the amplitude of the slosh motion. Solutions of these equations for a special case are discussed. An experiment was developed that systematically studied the nonlinear coupled motion for various fluid mass fractions, frequency ratios, and gravity levels. The experimental results verify and compliment the analytical model.

The paper is organized into five main sections. The first section briefly introduces the study model. The second and third sections present the analysis and the experiment. The results of the analysis and the experiment then are presented and discussed in the fourth section. The main points of the paper, suggested further research, and potential applications are summarized in the conclusion. More detailed explanations of both the analysis and the experiment can be found in Ref. 25 and the analytical method is detailed in Ref. 26.

Study Model and Coupled System Parameters

The study model, consisting of a spring-mass-damper spacecraft with fluid in a cylindrical tank, is conceptually simple, yet complex enough to embody the important nonlinear coupled effects (Fig. 1). A cylinder of dry mass m and radius $a = d/2$ is partially filled with fluid of density ρ and mass $m_F = \pi\rho a^2 h$. Motion of the tank in both the planar or lateral (x) direction and the nonplanar or transverse (y) direction are restrained by springs and dampers of strengths k_x and c_x, k_y and c_y. The mean gravity or acceleration vector $-g\hat{k}$ is aligned with the cylinder axis and is above the critical level necessary to collect the fluid to one end of the tank.[4]

Several nondimensional parameters govern the dynamics of this system. The nondimensional inertia scaling parameter is the mass ratio μ, the ratio of total fluid mass m_F to total dry mass m,

$$\mu = m_F/m \tag{1}$$

The nondimensional frequency scaling parameter is the frequency ratio ν, the ratio of the first slosh mode natural frequency in the linear limit ω_s to the tank undamped natural frequency ω_0. If the spring rates in the x and y directions are assumed equal to k, the frequency ratio is

$$\nu = \frac{\omega_s}{\omega_0} = \frac{\omega_s}{\sqrt{k/m}} \tag{2}$$

Because any nonlinear response of the fluid-spacecraft system will depend on the amplitude of the tank motion, it will depend on the magnitude of the applied force F_{ex} relative to the spring stiffness. The applied force F_{ex} therefore should be normalized by the spring rate k and the tank diameter d to give the following nondimensional force:

$$\Xi_{ex} = F_{ex}/kd \tag{3}$$

The fluid gravity force to capillary force ratio will determine the relative influence of the capillary forces. The usual normalization of the capillarity of the fluid free surface gives the Bond number Bo[4]

$$Bo = \rho g a^2/\sigma \tag{4}$$

in which ρ is the fluid density and σ the surface tension, and Bo determines the equilibrium free surface shape[27] and the linear slosh frequency ω_s.[1,4] Because Bo affects the basic geometry of the flow, it will effect the linear and nonlinear slosh modal masses and stiffnesses as well.

The damping ratios of the spacecraft mode ζ and the fluid slosh modes ζ_{qi} are assumed to be light (<0.10). The ζ_{qi} will depend on the fluid viscosity and Bo, and in general must be determined experimentally.

Analytical Fluid-Spacecraft Model

The analytical model is presented in the following three sections. First, the solution of the nonlinear kinematic boundary value problem is discussed, followed by the presentation of the coupled fluid-spacecraft Lagrangian and equations of motion. A solution of these equations for a special case is also presented.

Nonlinear Description of the Fluid Kinematics

The motion of the fluid is assumed to be inviscid, irrotational, and incompressible, and therefore the fluid velocity field relative to the tank $\boldsymbol{u}$ is uniquely defined by a three-dimensional flow potential $\phi(r,\theta,z,t)$, such that $\boldsymbol{u} = \nabla\phi$. The differential equation for ϕ is a statement of mass conservation for the fluid,

$$\nabla^2\phi = 0 \tag{5}$$

The boundary conditions on the free surface S_F and the wetted walls of the container are that the fluid velocity relative to the tank match the boundary velocity,[12,25]

$$\frac{\partial\eta}{\partial t} + \nabla\phi\cdot\nabla\eta = \frac{\partial\phi}{\partial z} \quad \text{on} \quad z = \eta \tag{6}$$

$$\frac{\partial\phi}{\partial r} = 0 \quad \text{on} \quad r = a \tag{7}$$

$$\frac{\partial\phi}{\partial z} = 0 \quad \text{on} \quad z = -h \tag{8}$$

in which $\eta(r,\theta,t)$ is the height of the free surface measured from the mean equilibrium height of the fluid h. It can be shown that Eqs. (7) and (8) are both special cases of Eq. (6).[25] The free surface boundary condition [Eq. (6)] is the source of the convection nonlinearity in the fluid motion.[12]

The solution of the Dirichlet boundary value problem given by Eqs. (5–8) will be a unique and complete specification of the fluid flowfield.[12,25] Although there is no known exact solution to this nonlinear boundary value problem, Miles[12] showed that this problem can be solved approximately by satisfying the first-order stationary conditions for the following integral:

$$S_B I = \tfrac{1}{2}\iiint_V (\nabla\phi)^2\,\mathrm{d}V - \iint_{S_B}\phi(z=\eta)\dot{\eta}\,\mathrm{d}S_B \tag{9}$$

in which $S_B = \pi a^2$ is the (r,θ) cross section of the container. In Ref. 25, it was shown that this is also true even for a curved

free surface, and therefore it can be applied to the low-gravity case by extending the approach of Miles.[12]

To obtain an approximate solution to Eqs. (5–8), the following modal expansions are introduced for the fluid flow potential ϕ and the free surface motion η:

$$\phi(r,\theta,z,t) = \sum_{n=1}^{N} \frac{\cosh[k_n(z+h)]}{\cosh(k_n h)} \psi_n(r,\theta)\phi_n(t) \tag{10}$$

$$\eta(r,\theta,t) = f(r,\theta) + \sum_{n=1}^{N} \xi_n(r,\theta)q_n(t) \tag{11}$$

where N is the number of assumed modes. At this point, N is considered to be arbitrarily large but will later be fixed to a finite number of assumed fluid modes. The free surface equilibrium shape $f(r,\theta)$ is a function of Bo and the fluid-container contact angle α.[4] In the limit of very large gravity, $Bo \to \infty$, the equilibrium free surface is flat, and $f \to 0$. For arbitrary Bo, $f(r,\theta)$ must be calculated numerically.[27] The k_n are the radial wave numbers for the ψ_n mode shapes of the internal fluid flow given by the solution to the following eigenvalue problem:

$$\nabla^2\psi_n + k_n\psi_n = 0 \qquad \text{on} \quad S_B \tag{12}$$

$$\frac{\partial\psi_n}{\partial r} = 0 \qquad \text{on} \quad r = a \tag{13}$$

$$\iint_{S_B} \psi_i\psi_j \, dS_B = \delta_{ij}S_B \tag{14}$$

The ξ_n free surface mode shapes satisfy a similar eigenvalue problem,

$$\nabla^2\xi_n + k_n\xi_n = 0 \qquad \text{on} \quad S_B \tag{15}$$

$$\frac{\partial\xi_n}{\partial r} = \frac{\Gamma}{a}\xi_n \qquad \text{on} \quad r = a \tag{16}$$

$$\iint_{S_B} \xi_i\xi_j \, dS_B = \delta_{ij}S_B \tag{17}$$

in which Γ is a linear contact angle hysteresis constant.[4,9] Note that, except in the case $\Gamma = 0$, ψ_n and ξ_n will not be equal. These particular modal expansions [Eqs. (11) and (10)] satisfy Eqs. (5), (7), and (8) identically. They also encompass not only circular cylindrical tank cross sections with flat bottoms but also arbitrary cross section shapes, so long as the walls are vertical, and arbitrary bottom shapes, if the deviation from a flat bottom is much less than the total depth of the fluid h. A further refinement could be made by restricting the ξ_n to satisfy the boundary condition given by a linearization of Eq. (6). In general, these must be calculated numerically via one of the existing linear analysis methods.[4,6–8]

Proceeding as in Miles,[12] the above expansions for η and ϕ are substituted into the variational statement, Eq. (9). After considerable algebra (detailed in Ref. 25), the potential generalized coordinates ϕ_n are related to the free surface generalized coordinates q_n by the following nonlinear relation:

$$\phi_m = \sum_{n=1}^{N} \ell^{(0)}_{mn}\dot{q}_n + \sum_{n=1}^{N}\sum_{r=1}^{N} \ell^{(1)}_{mnr}q_r\dot{q}_n + \sum_{n=1}^{N}\sum_{r=1}^{N}\sum_{s=1}^{N} \ell^{(2)}_{mnrs}q_rq_s\dot{q}_n \tag{18}$$

plus terms of higher than cubic order in the free surface displacement. This equation is an approximate solution to the nonlinear boundary value (kinematic) problem [Eq. (6)] and, through Eq. (10), expresses the motion of the fluid relative to the tank in terms of the generalized coordinates q_n. The coefficients $\ell^{(0)}_{mn}$, $\ell^{(1)}_{mnr}$, and $\ell^{(2)}_{mnrs}$ are complicated functions of integrals of the assumed mode shapes and are given in Refs. 25 and 26. Physically, they are generalized nonlinear corrections to the modal wavelength. It is interesting to note that the ϕ_m are generalized speeds for the fluid motion and Eq. (18) is a nonlinear kinematic equation for the fluid motion derived from the boundary conditions of the flow.

System Lagrangian and Equations of Motion

Using the kinematic description of Eq. (18), a coupled system Lagrangian can be constructed in terms of the fluid generalized coordinates $q_n (n = 1,2,...,N)$. The fluid kinetic energy is the volume integral of the absolute velocity of the fluid particles $\dot{x}$ times the mass density ρ,

$$T_F = \tfrac{1}{2}\iiint_V \rho\dot{x}\cdot\dot{x} \, dV = \tfrac{1}{2}\iiint_V \rho[\dot{R} + \nabla\phi]\cdot[\dot{R} + \nabla\phi] \, dV \tag{19}$$

in which $\dot{R} = \dot{x}\hat{\imath} + \dot{y}\hat{\jmath}$, the coordinates of the tank in inertial space. Expanding the dot product, employing Green's Theorem to reduce the volume integral to a surface integral, substituting the modal expansion [Eq. (10)] and the kinematics [Eq. (18)], and truncating to terms of order $(q_n)^4$ results in the following expression for T_F[25]:

$$\begin{aligned} T_F = {} & \tfrac{1}{2}m_F(\dot{x}^2 + \dot{y}^2) \\ & + \tfrac{1}{2}\rho S_B \sum_{m=1}^{N}\sum_{n=1}^{N} a^{(0)}_{mn}\dot{q}_m\dot{q}_n \\ & + \tfrac{1}{2}\rho S_B \sum_{m=1}^{N}\sum_{n=1}^{N}\sum_{r=1}^{N} a^{(1)}_{mnr}q_r\dot{q}_m\dot{q}_n \\ & + \tfrac{1}{2}\rho S_B \sum_{m=1}^{N}\sum_{n=1}^{N}\sum_{r=1}^{N}\sum_{s=1}^{N} a^{(2)}_{mnrs}q_rq_s\dot{q}_m\dot{q}_n \\ & + \rho\dot{x}\left(\sum_{n=1}^{N}\dot{q}_n\iint_{S_B}\xi_n r\cos\theta \, dS_B\right) \\ & + \rho\dot{y}\left(\sum_{n=1}^{N}\dot{q}_n\iint_{S_B}\xi_n r\sin\theta \, dS_B\right) \end{aligned} \tag{20}$$

The first term is the kinetic energy for the fluid moving as a solid mass. The second, third, and fourth terms are the linear, quadratic, and cubic slosh mass terms. The a_{mn} coefficients, which are complicated functions of the kinematic integrals of the assumed mode shapes,[25,26] form the "equivalent slosh depth" matrix, which determines the equivalent height of fluid participating in the motion of the mn modal motion. The last two terms in Eq. (20) result from cross terms in the expansion of the dot product in Eq. (19). They are the coupling between the motion of the tank and the motion of the fluid inside. Note that, for this case, in which the tank translates but does not rotate, these terms are quadratic, and therefore the equations of motion will be linearly coupled. As noted in Ref. 25, this is not the case if pitching motion were included. It also should be noted that this expression for T_F reduces to that of Miles[12] when the free surface is flat ($f = 0$).

The potential energy of the fluid has two components. The first, due to the action of gravity, is given by

$$U_G = \iiint_V \rho gz \, dV = \frac{\rho g S_B}{2}\sum_{i=1}^{N} q_i^2 \tag{21}$$

The other contribution to the fluid potential energy is the surface tension energy, which, for constant surface tension σ is[18]

$$U_\sigma = \sigma\iint_{S_B}\sqrt{1 + \nabla\eta\cdot\nabla\eta} \, dS_B \tag{22}$$

Table 1 Assumed Bessel function fluid mode shapes for the analytical fluid-spacecraft model

Modal index	Name	Order	ψ_i	ξ_i	Nodal diam
1	Planar primary	ϵ	$A_{11}J_1(k_{11}r)\cos(\theta)$	$B_{11}J_1(\lambda_{11}r)\cos(\theta)$	1
2	Nonplanar primary	ϵ	$A_{11}J_1(k_{11}r)\sin(\theta)$	$B_{11}J_1(\lambda_{11}r)\sin(\theta)$	1
3	Axisymmetric secondary	ϵ^2	$A_{01}J_0(k_{01}r)$	$B_{01}J_0(\lambda_{01}r)$	0
4	Planar secondary	ϵ^2	$A_{21}J_2(k_{21}r)\cos(2\theta)$	$B_{21}J_2(\lambda_{21}r)\cos(2\theta)$	2
5	Nonplanar secondary	ϵ^2	$A_{21}J_2(k_{21}r)\sin(2\theta)$	$B_{21}J_2(\lambda_{21}r)\sin(2\theta)$	2

Substituting the modal expansion [Eq. (11)] into this expression and again keeping only terms of order $(q_n)^4$ or less results in

$$U_\sigma = \sigma S^{(0)} + \sigma \sum_{i=1}^{N} S_i^{(1)} q_i + \sigma \sum_{i=1}^{N}\sum_{j=1}^{N} S_{ij}^{(2)} q_i q_j + \sigma \sum_{i=1}^{N}\sum_{j=1}^{N}\sum_{k=1}^{N} S_{ijk}^{(3)} q_i q_j q_k + \sigma \sum_{i=1}^{N}\sum_{j=1}^{N}\sum_{k=1}^{N}\sum_{l=1}^{N} S_{ijkl}^{(4)} q_i q_j q_k q_l \tag{23}$$

The S_{ij} are coefficients in a Taylor series expansion for the instantaneous free surface area.[25,26] When $f=0$, the above coefficients reduce to analogous terms derived by Limarchenko.[15,18] The cubic coefficients $S_{ijk}^{(3)}$ are not present in Limarchenko's derivation, primarily because of the perturbation there about a flat free surface equilibrium shape. As a consequence, the Limarchenko equations of motion exclude very important cubic coupling terms, which are included in this derivation.

While the above energy expressions are valid for any number of generalized coordinates, a proper analytical model need only include enough modes to predict the correct nature of the nonlinear response. In this analysis, five fluid modes are retained in the fluid representation, as also done by Miles.[13,14] Table 1 lists the definitions of these assumed mode shapes. The first two modes are termed *primary* modes and correspond to q_1 and q_2. The generalized coordinate q_1 corresponds to the eigenmode for $\cos(\theta)$, the planar primary fluid mode, and q_2 corresponds to the eigenmode for $\sin(\theta)$, the transverse or nonplanar primary fluid mode. Superposition of q_1 and q_2 produces rotary motion in the fluid. Only the first three higher-frequency modes are retained: q_3, q_4, and q_5. These higher-order modes are termed *secondary* modes. The mode shape for q_3 is axisymmetric, that for q_4 corresponds to $\cos(2\theta)$, and that for q_5 corresponds to $\sin(2\theta)$.

These modes have been chosen by truncating the modal expansions to include only modes that significantly affect the nonlinear equations of motion. To do this, a perturbation parameter ϵ is introduced that has a magnitude of the order of the motion of the tank and therefore can be based on the magnitude of the applied force Ξ_{ex}. For impulsive excitation, ϵ will be such that $\Xi_{ex} = \epsilon\delta(t)$. For harmonic resonant excitation, ϵ will be such that $\Xi_{ex} = \epsilon^3\cos(\Omega t)$.

Using the assumed perturbation parameter ϵ, the importance of the fluid modes to the motion can be compared. For systems with frequency ratios v near 1, the fluid motion in the first fluid mode q_1 will be of order ϵ. If transverse (nonplanar) fluid motion is excited, the nonplanar fluid mode q_2 will also be of order ϵ. All other fluid modes will be of order ϵ^2 or less. Following an argument first presented by Miles,[13] modal coordinates that contribute terms of order ϵ^3 or less to the equations of motion must be retained. This does not imply that the fluid modes of order ϵ^2 can be ignored in the modal expansion. Modal coordinates of order ϵ^2 can multiply modal coordinates of order ϵ to produce cubic order forces in the equations of motion. In fact, as previously discussed in Refs. 11–14, higher-order fluid modes must always be retained to predict the nonlinear response of the first-order modes properly. As noted in Ref. 25, an assumed mode model that includes only the first-order mode q_1 predicts a fluid vibration frequency that increases with amplitude rather than decreases, as is observed experimentally. Therefore, retaining higher-order modes is necessary not only quantitatively but also qualitatively. As noted before by Miles,[13] all order ϵ^2 modes other than q_3, q_4, and q_5 will either not couple to the cubic order motion of the primary modes or will have dynamic coefficients numerically much smaller than those for the secondary modes retained in this model.

For this set of assumed modes, the fully coupled, cubic order nonlinear Lagrangian for the fluid-spacecraft motion is[25]

$$\begin{aligned} L = {} & \tfrac{1}{2}m_F(\dot{x}^2+\dot{y}^2) + m_{xq}\dot{x}\dot{q}_1 + m_{yq}\dot{y}\dot{q}_2 \\ & + \tfrac{1}{2}m\dot{x}^2 + \tfrac{1}{2}m\dot{y}^2 - \tfrac{1}{2}k_x x^2 - \tfrac{1}{2}k_y y^2 + \tfrac{1}{2}\rho S_B\Bigg[\sum_{m=1}^{5} a_{mn}^{(0)}\dot{q}_m^2 \\ & + \sum_{m=1}^{2}\sum_{n=1}^{2}\sum_{r=3}^{5}(a_{mnr}^{(1)}q_r\dot{q}_m\dot{q}_n + 2a_{rmn}^{(1)}q_n\dot{q}_r\dot{q}_m) \\ & + \sum_{m=1}^{2}\sum_{n=1}^{2}\sum_{r=1}^{2}\sum_{s=1}^{2} a_{mnrs}^{(2)}q_r q_s\dot{q}_m\dot{q}_n\Bigg] \\ & - \tfrac{1}{2}\rho g S_B\sum_{i=1}^{5} q_i^2 - \sigma\sum_{i=1}^{5} S_{ii}^{(1)}q_i^2 \\ & - \sigma\sum_{i=1}^{2}\sum_{j=1}^{2}\sum_{k=3}^{5}(2S_{ijk}^{(3)} + S_{kji}^{(3)})q_i q_j q_k \\ & - \sigma S_{1111}^{(4)}q_1^4 - \sigma S_{1111}^{(4)}q_2^4 \\ & - \sigma(S_{1122}^{(4)} + S_{2211}^{(4)} + 4S_{1212}^{(4)})q_1^2 q_2^2 \end{aligned} \tag{24}$$

in which the coupling coefficients are

$$m_{xq} = \iint_{S_B}\xi_1 r\cos\theta\, dS_B, \quad m_{yq} = \iint_{S_B}\xi_2 r\sin\theta\, dS_B \tag{25}$$

Seven nonlinear equations of motion result from this Lagrangian for the fluid-spacecraft degrees of freedom, x, y, q_1, q_2, q_3, q_4, and q_5. Solutions of these equations are, in general, very complicated and the subject of current research. A substantially simpler special case can be found from considering the motion of the fluid-spacecraft system below the amplitude necessary to generate nonplanar motion. Because the excitation F_{ex} is only in the planar (x) direction, the coupled motion at infinitesimal (linear) amplitudes will remain planar. The nonlinear departure from the linear motion at intermediate amplitudes will likewise remain planar. In this case, the nonplanar fluid mode q_2 and the nonplanar spacecraft degree of freedom y are zero. Furthermore, the third secondary fluid mode q_5 no longer participates in the motion. By applying Lagrange's equations to the resulting form of Eq. (24), the following set of equations of motion are found, which apply so long as the fluid slosh motion is completely planar:

Spacecraft motion:

$$(1+\mu)\ddot{x} + \mu_{xq}\ddot{q}_1 + 2\zeta\dot{x} + x = \Xi_{ex} \tag{26}$$

Primary fluid mode:

$$\frac{\lambda\mu}{\mu_{xq}}\ddot{x} + \ddot{q}_1 + 2\zeta_{q1}v\dot{q}_1 + v^2 q_1 + \alpha_{113}(\dot{q}_3\dot{q}_1 + q_3\ddot{q}_1) + \alpha_{311}q_1\ddot{q}_3 + \alpha_{114}(\dot{q}_4\dot{q}_1 + q_4\ddot{q}_1) + \alpha_{411}q_1\ddot{q}_4 + v^2\beta_{113}q_1q_3 + v^2\beta_{114}q_1q_4 + \alpha_1(q_1\dot{q}_1^2 + q_1^2\ddot{q}_1) + v^2\beta_1 q_1^3 = 0 \quad (27)$$

Axisymmetric secondary fluid mode:

$$\mu_{33}(\ddot{q}_3 + 2\zeta_{q3}v_3\dot{q}_3 + v_3^2 q_3) + (\alpha_{311} - \tfrac{1}{2}\alpha_{113})\dot{q}_1^2 + \alpha_{311}q_1\ddot{q}_1 + \tfrac{1}{2}v^2\beta_{113}q_1^2 = 0 \quad (28)$$

Planar secondary fluid mode:

$$\mu_{44}(\ddot{q}_4 + 2\zeta_{q4}v_4\dot{q}_4 + v_4^2 q_4) + (\alpha_{411} - \tfrac{1}{2}\alpha_{114})\dot{q}_1^2 + \alpha_{411}q_1\ddot{q}_1 + \tfrac{1}{2}v^2\beta_{114}q_1^2 = 0 \quad (29)$$

These equations have been scaled so that displacements are in units of tank diamater d, time is in units of spring-mass periods $1/\omega_s$. Surface tension σ has been properly scaled in terms of Bo, and the expression for ω_s has been used to scale gravity g. The coefficients α_i,α_{ijk} are nondimensional versions of the a_{mn}; similarly, the β are nondimensional versions of the S coefficients in U_σ. The μ_{ii} and v_i are nondimensional inertia and frequencies for the secondary modes.

One approximate solution of these equations that is near the linear solution can be found through application of the multiple time scales perturbation technique.[28] In this method, the generalized coordinates are expanded in the following perturbation series:

$$\begin{aligned} x &= \epsilon x_1(T_0,T_2) + \epsilon^3 x_3(T_0,T_1) \\ q_1 &= \epsilon q_{11}(T_0,T_2) + \epsilon^3 q_{13}(T_0,T_1) \\ q_3 &= \epsilon^2 q_{32}(T_0) \\ q_4 &= \epsilon^2 q_{42}(T_0) \end{aligned} \quad (30)$$

in which the independent time scales are $T_i = \epsilon^i t$. The substitution of these perturbations into the equations of motion results in first-, second-, and third-order perturbation equations that are then solved in sequence. These are detailed in Ref. 25.

The most important intuitive result of this perturbation solution concerns the role of the secondary fluid modes in the coupled motion. As expected from a linear analysis, x and q_1 couple together to form two fluid-spacecraft eigenmodes, with eigenfrequencies v_1 and v_2. However, the motion of these fluid-spacecraft eigenmodes are nonlinearly coupled to not only q_1 but also the secondary modes q_3 and q_4. In fact, resonances between the fluid-spacecraft eigenmodes and q_3 and q_4 determine the nonlinear corrections to v_1 and v_2. They also lead to singular conditions of the analytical model for certain eigenfrequencies. These can occur when a secondary fluid modal frequency (either v_3 or v_4) coincides with twice either eigenfrequency ($2v_1$ or $2v_2$), with the sum of the eigenfrequencies ($v_1 + v_2$), or with the difference of the eigenfrequencies ($v_1 - v_2$). This greatly contrasts with the nonlinear uncoupled motion of the fluid. As discussed by Miles,[13,14] internal resonance singularities between the uncoupled primary fluid modes and the secondary fluid modes occur only for a very shallow quiescent depth h. For the coupled fluid-spacecraft system, however, these internal resonances can develop at any fluid depth and depend on the fluid-spacecraft eigenfrequencies v_1 and v_2. They therefore depend on the coupled fluid-spacecraft parameters μ, v, and Bo.

Experimental Investigation

The experimental objectives of this research were to provide quantitative confirmation of the restricted planar analytical model developed above and to provide qualitative evidence of how the coupled fluid-spacecraft system behaves when the fluid is allowed to execute nonplanar motion. An experimental model of the study model system was developed in which the motion of the spacecraft was restricted to the planar (x) direction, but the fluid was allowed general planar and nonplanar motion. The nonlinear response of dynamically similar scale model fluid spacecraft systems were characterized as a function of nondimensional excitation Ξ_{ex}. The coupled system mass ratio μ, frequency ratio v, and the Bond number Bo, were systematically varied so as to generate experimental test data that demonstrated the parametric effects on the observed nonlinear coupled motions and that could be compared to the analytical model. The fluid height h was kept equal to the tank diameter d.

Low Bond numbers were achieved using small containers[9] in 1 g and similar scale models in 0 g in parabolic flight tests, as shown in Table 2. Bond numbers of 33 and 58 were obtained in 1 g using water as a modeling fluid in 3.1 and 4.1 cm diameter Pyrex glass tanks. Because previous investigations[4,9] have noted difficulty predicting the natural frequency of water in glass due to a particularly high contact line hysteresis level Γ, a series of test results were obtained in 1 g using a 2% photoflo-water solution in a 3.1 cm diameter Pyrex glass. Photoflo is a surfacant that reduces σ by a factor of two, giving a Bond number of 66. In addition, photoflo reduces the fluid-container contact angle α to zero and reduces the contact angle hysteresis constant Γ to zero. Bond numbers less than 20–30 cannot be modeled in 1 g because the slosh damping becomes unacceptably high.[9] For this reason, a Bond number of zero was obtained in 0 g parabolic flight tests on the NASA KC-135 Reduced Gravity Test Facility. Typical rms gravity levels of 0.01 g for periods of 20–25 s are maintained in this facility. Because of the gravity settling time, the transient impulse response tests were more successful and more efficient in 0 g than harmonic resonance tests in 0 g.

The use of small-scale fluid model tanks required the development of a unique experimental apparatus to generate a coupled fluid-spacecraft system. This apparatus, called a compliant actuator, is discussed in detail in Ref. 25 and is briefly described here (Fig. 2). The model fluid tank was supported by a sensitive deterministic force reaction balance that mea-

Table 2 Simulated Bond numbers studied in this research with identified linear limit slosh frequencies, damping ratios, and hysteresis constants

Fluid dynamic test condition				Identified planar slosh mode parameters		
d, cm	g	Fluid	Bo	$\omega_s/2\pi$, Hz	ζ_{q1},%	Γ
3.1	1.0	Photoflo	66	5.43	3.49	0
4.1	1.0	Water	58	5.28	4.20	−5.0
3.1	1.0	Water	33	6.65	4.64	−7.8
4.1	0.01	Water	~0	2.05	22.8	−9.8

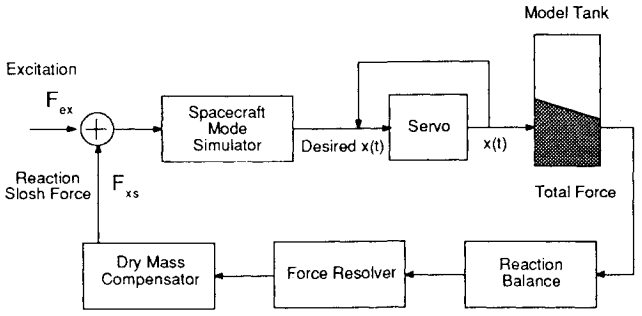

Fig. 2 Component block diagram of the compliant actuator spacecraft mode simulator.

sured three support forces eccentric to the center of mass at 120 deg intervals. In the "force resolver," the force components in the horizontal plane (F_x,F_y,M_z) were resolved by an analog electronic matrix transformation of the transducer force signals. In the "dry mass compensator," the dry mass inertia force contributions were removed electronically by addition of a signal equal to the measured acceleration of the tank support times the known system dry mass. After removing the dry mass inertia force from the measurement, only the reaction slosh forces F_{xs} and F_{ys} remained. The reaction slosh force measurement in the planar direction F_{xs} served as the input to the analog computer ("spacecraft mode simulator"), which solved the differential equation for the spacecraft motion,

$$m\ddot{x} + c\dot{x} + kx = F_{ex} + F_{xs} \tag{31}$$

The excitation force F_{ex} was provided by an electronic waveform generator. The output of the analog computer, a voltage proportional to the spacecraft motion x, drove the motion of the tank through a servoshaker system. Using this system to simulate and drive the model tank lateral motion, the fluid slosh was coupled to the motion of the tank. By adjusting the feedback gains in the analog computer, the simulated spacecraft modal mass, damping, and frequency could be adjusted independently. This method greatly increased the experimental fluid mass fractions that were possible and enabled precise adjustment of the spacecraft modal dynamics.

For each of the 4 Bond numbers simulated in this research, a total of 11 different scaled coupled systems were studied, each characterized by a particular combination of μ, ν, and ζ. Mass ratios between 0.12 and 0.41 were studied at frequency ratios near 0.80, 1.0, and 1.2 times the frequency ratio predicted to produce the closest tuning in the eigenfrequencies for the particular mass ratio. For each of these 44 different systems, impulsive free decays were studied at three values of excitation Ξ_{ex}. Resonance response sweeps at five different amplitudes of Ξ_{ex} were generated for the coupled systems with $\mu = 0.16$ and 0.41 at each of the four Bo levels.

Analytical and Experimental Results

The analytical and experimental results of this research are presented in three subsections. In the first, the uncoupled response of the fluid to prescribed lateral motion of the tank is briefly presented. The second introduces and generalizes the important analytical and experimental results of this research. The third presents typical experimental and analytical results that illustrate the important characteristics of nonlinear coupled fluid-spacecraft motion.

Uncoupled Response of the Fluid to Prescribed Motion of the Tank

While experimental observations of the uncoupled fluid response have been extensively reported in the literature,[1,11] it is important to document the behavior for the combinations of fluids and Bond numbers used in this research. The uncoupled slosh behavior as a basis for discussing the nonlinear coupled response. Particularly unique aspects of this experimental data not presented before are the observation of capillary effects on the nonlinear motion and the measurement of the nonplanar slosh force F_{ys} as well as the usually observed planar slosh force F_{xs}.

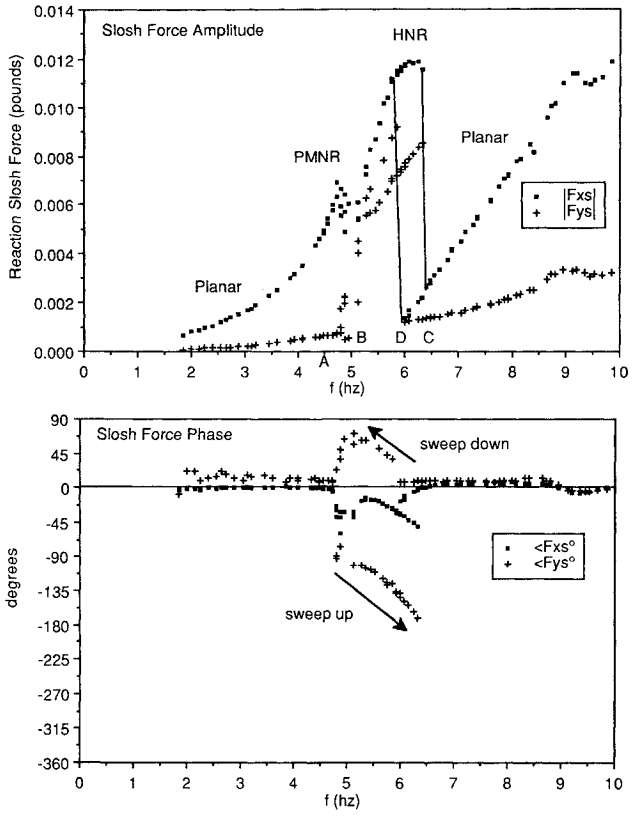

Fig. 3 Uncoupled fluid resonance for $Bo = 66$, photoflo test condition and lateral harmonic motion of $x/d = 0.0270$. Three types of nonlinear fluid motion are observed.

The principal observations of the uncoupled fluid response made in this research are the following:

1) As expected, a linear model of the fluid slosh is very precise at very low slosh wave amplitudes. Linear slosh parameters were identified for incorporation into the nonlinear analytical model and are listed in Table 2.

2) At moderate amplitudes, the natural frequency of the slosh decreases with amplitude of the motion.

3) At large amplitudes, several resonant slosh motions are possible, as described in the existing literature.

4) As the Bond number is decreased, the uncoupled slosh motion becomes more nonlinear and more strongly linked to the motion of the higher-frequency secondary modes.

5) The 0 g zero Bond number uncoupled parabolic flight test data demonstrated a strong correlation between the natural frequency of the slosh motion and the measured transient gravity level.

Figure 3 presents a typical, large amplitude, reaction slosh force resonance curve for the uncoupled fluid response for the photoflo, $Bo = 66$ test condition. In this example, the tank is harmonically excited at a constant amplitude of 0.0270 tank diameters. Below the natural slosh frequency (A), the fluid moves only in a planar motion and the nodal diameter line of the free surface motion is perpendicular to the motion of the tank. Only F_{xs} is nonzero in this region. Just below the natural slosh frequency (at A), higher harmonics in the reaction slosh force (indicating the excitation of the secondary fluid modes) become strong, and nonplanar motion of the fluid becomes unstable (F_{ys} becomes nonzero). In this narrow region of excitation frequency, the type of motion is designated periodically modulated nonplanar resonance (PMNR). In PMNR, the nodal diameter line of the slosh motion is no longer perpendicular to the motion of the tank, but oscillates

both clockwise and counterclockwise in multiples of the excitation frequency. Miles[14] indicated that chaotic motions of the node line are possible in this region, but this was not observed. At a distinct frequency (B), the nonplanar motion of the fluid becomes harmonic, and the fluid begins to rotate. This motion is designated harmonic nonplanar resonance (HNR). In HNR, F_{xs} and F_{ys} are approximately equal in magnitude and differ in phase by 90 deg. As the excitation frequency passes another critical frequency (C), the nonplanar motion jumps back to a purely planar motion. (The nonplanar reaction slosh force measured above C is experimental error.) When the excitation frequency is swept down from above the resonance, HNR begins at a slightly lower frequency (D) than it ended for the sweep up, demonstrating a hysteresis in the resonance jump, as is often characteristic of a nonlinear system. It is important to realize that the absolute value of the phase of F_{ys} is different during HNR in the sweep up and the sweep down. In both cases, the phase with respect to F_{xs} is approximately 90 deg, but one motion corresponds to clockwise rotation of the fluid and one to counterclockwise rotation of the fluid. The different directions of rotation are dynamically equivalent, and both are equally possible. In fact, it was observed experimentally that there was little or no preference for the direction of fluid rotation during HNR. Furthermore, the directions of rotation were not always different in different resonance tests of the same fluid-tank combination.

General Observations of the Coupled Fluid-Spacecraft Response

With the preceding discussion of the nonlinear uncoupled fluid slosh behavior as necessary background, the important observations about the nonlinear coupled fluid-spacecraft motion will now be highlighted. The principal conclusions supported by the analysis and experiment of this research concerning the coupled fluid-spacecraft dynamics are the following:

1) The motion of an otherwise linear spacecraft mode, when coupled to the motion of a contained sloshing fluid, can exhibit strongly nonlinear dynamics when the frequency of the slosh motion and the spacecraft mode nearly coincide.

2) The nonlinear coupled fluid-spacecraft motion can be predicted only by a coupled analytical model. A linear coupled model or a nonlinear uncoupled fluid model will predict motion completely unlike what is observed experimentally.

3) The coupled nonlinear fluid-spacecraft motion exhibits types of resonance motions not found in the uncoupled nonlinear motion of the fluid. Superposition does not apply for a nonlinear system even when part of the system is linear. Uncoupled nonlinear models of the fluid slosh that neglect the important internal resonance effects will not correctly predict these new types of motions.

4) Convection nonlinearities are important at all Bond numbers, but capillary nonlinear effects on the coupled nonlinear fluid-spacecraft motion must be modeled for Bond numbers as high as 60–100.

5) The nonlinearity in the coupled fluid-spacecraft system is strongest for coupled systems with frequency ratios ν of 0.6–1.2 and for coupled systems with mass ratios μ of 0.1–0.2. The coupled nonlinear response will be strongest when a linear coupled model predicts the closest linear eigenfrequencies ν_1 and ν_2.

These observations are further elaborated in the remainder of this subsection and are illustrated by typical quantitative results in the next.

As expected, the response to very low levels of excitation of all the coupled systems tested in this research were very accurately modeled using a linearized model of the fluid. The extent of motions that could be accurately modeled as linear, however, was very limited. This departure from the prediction of a linear model will be discussed using first the impulsive free decay nonlinear coupled behavior and then the resonance nonlinear coupled behavior.

At the beginning of the free decays, the fluid-spacecraft natural frequencies are shifted from their linear values in proportion to the square of the amplitude of the initial condition. Such *decreasing* frequency with amplitude is usually termed *softening* nonlinear behavior, even though in this system the physical mechanisms responsible for the frequency shift are more complicated than that of a simple nonlinear softening spring. The observed frequency shifts were very large. Coupled fluid-spacecraft systems with initial spacecraft modal displacements of 0.02 tank diameters had eigenfrequencies which were 10% less than the linearly predicted values. This effect will be exaggerated in a full-scale system with lighter slosh damping ratio ζ_{qi}.

The coupled fluid-spacecraft natural frequencies also change during the free decay. As the motion amplitude decays due to damping, the vibration eigenfrequencies approach their linearized values. The time constant of the eigenfrequency shift was half that of the damping time constant, confirming that the nonlinear vibration frequencies differ from the linear values in proportion to the square of the amplitude of the motion.

Simple nonlinear softening behavior was not always observed. Coupled systems near one of the internal secondary fluid mode resonances (discussed above) exhibited an apparent saturation phenomenon for which the eigenfrequencies cease to depend on the amplitude of the motion above a certain value. The motion of such systems could be modeled only by considering the secondary modes to be of order ϵ instead of ϵ^2 as assumed above. Furthermore, the analytical model predicts that, just as in uncoupled nonlinear slosh,[14] the system eigenfrequencies decrease or increase with amplitude of the motion depending on the resonance of the secondary modes. In fact, the resonance of the secondary modes (especially at low *Bo*) is so prevalent for any fluid depth in the coupled systems, whether the system eigenfrequencies increase or decrease with amplitude can change simply by perturbing the frequency ratio ν by a few percent.

The harmonic resonance of the coupled systems studied also exhibited a softening nonlinear behavior. Harmonic system resonances with tank motions greater than 0.005 diam had resonance peaks 5–10% below their linear values. For tank motion amplitudes greater than 0.01 diam, however, the harmonic response of the coupled system exhibited some of the multiply stable and nonplanar motions previously observed in the uncoupled fluid slosh. Ordinary planar resonance, PMNR, and HNR were observed at all the 1 g Bond numbers studied. In a coupled system undergoing PMNR, the spacecraft motion x as well as the slosh motion are periodically modulated. Jump and hysteresis, which likewise included both the spacecraft and the slosh motion, were also observed.

The types of resonances observed in the experimental coupled fluid-spacecraft resonances were not limited, however, to those previously observed in the nonlinear uncoupled fluid resonance. At least three additional stable resonant nonlinear coupled responses were also observed: a secondary planar resonance, a skewed nonplanar motion, and a completely unsymmetrical periodically modulated fluid-spacecraft motion. That these three types of motion are absent in the nonlinear uncoupled response of the fluid underscores the fact that the behavior of a coupled system composed of a linear subsystem and a nonlinear subsystem is not necessarily predicted by the behavior of the nonlinear subsystem alone. Furthermore, it appears likely that these types of behavior are strongly linked to the internal resonance with the secondary fluid modes. The number of internal resonances in the coupled system are eight and occur at all fluid depths, while in the uncoupled fluid motion there are only two, which occur only at shallow fluid depths. This may explain, in part, the extraordinary complexity of the coupled nonlinear fluid-spacecraft resonance.

Nonlinear coupled fluid-spacecraft behavior is more pronounced when the linear coupled system eigenfrequencies (ν_1

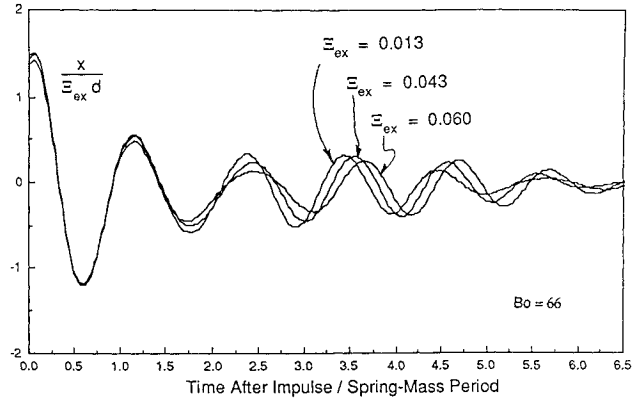

Fig. 4 Normalized free decay response in the spacecraft degree of freedom x for the coupled system ($Bo = 66$, $\mu = 0.16$, $\nu = 1.07$, $\zeta = 9.5\%$, photoflo) at three values of initial impulse amplitude Ξ_{ex}.

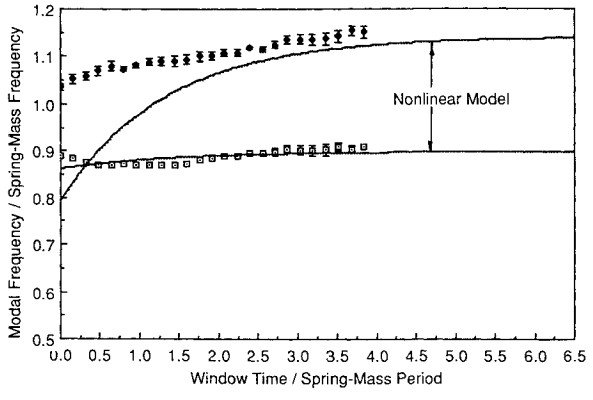

Fig. 5 Windowed ERA identifications for the largest of the free decays of Fig. 4 ($\Xi_{ex} = 0.060$). Nonlinear theory from the planar analysis is overplotted.

and ν_2) are closer together. In this condition, a given external force applied to the spacecraft mode will more easily resonate motion in the fluid. This always leads to a more nonlinear coupled fluid-spacecraft response. A very important result comes from this observation. The linear coupled system eigenfrequencies are closest together when the frequency ratio ν is approximately 1 *and* the fluid mass ratio μ is arbitrarily small. Therefore, coupled systems with lighter fluid mass fractions are potentially more nonlinear than systems with heavy mass fractions. Conversely, the mass fraction of fluid μ must be sufficiently large for the slosh force to affect the motion of the spacecraft. There will therefore be a medium range of fluid mass fractions, apparently between 0.10 and 0.20, for which the motion of the spacecraft is most nonlinear. The analytical model predicts this directly, and the experiment confirmed this result.

Any nonlinear model of fluid-spacecraft motion must a priori include the action of the secondary fluid modes in the formulation of the fluid dynamic model. Single-mode, nonlinear representations of the fluid (such as pendulum models) are physically incomplete: they possess too few degrees of freedom to predict the coupled fluid-spacecraft motion accurately. It should be especially noted that the nonlinear motion of a pendulum and the uncoupled nonlinear fluid slosh, although similar in response under some conditions, are driven by fundamentally different nonlinearities. A pendulum has an amplitude-dependent restoring spring force, while nonlinear slosh is controlled primarily by an amplitude-dependent mass convection effect involving higher-frequency modes.

Although the important nonlinear motions discussed above are present at all Bond numbers, capillarity increases the nonlinearity in the fluid-spacecraft system at lower Bond numbers. These effects were observed in all three 1 *g* *Bo* levels and were partially confirmed in the 0 *g* parabolic flight test experiments. Two physical mechanisms contribute to the effect of capillarity on the nonlinear coupled fluid-spacecraft motion. The first, more direct effect is that of the nonlinear capillary contribution to the fluid potential energy U_σ in Eq. (22). The second effect is an indirect effect through the action of the secondary fluid modes on the nonlinear fluid-spacecraft motion. Because the secondary fluid modes have shorter wavelengths, their linear limit natural frequencies ν_3, ν_4, and ν_5 are more sensitive to capillarity than the primary fluid modal frequencies. Their frequencies are affected at Bond numbers as high as 60–100, while the primary modes are not affected for *Bo* much higher than 20. It is the resonance of these secondary fluid modes that determines most of the nonlinear fluid-spacecraft response. Therefore, the nonlinear fluid-spacecraft dynamics are affected by capillarity for Bond numbers at which the linearized fluid-spacecraft dynamics would be unaffected. Furthermore, the number of internal secondary modal resonances within the critical range of ν *increases* as *Bo* approaches zero. At a Bond number of 0, the number of secondary fluid modal resonances present in the critical range is so dense and are so intense that, for almost any coupled fluid-spacecraft system near $Bo = 0$, the secondary modes must be considered *first-order modes*. At zero gravity, the nonlinear coupled motion becomes even more complicated than at moderate to high *Bo*. This analytically predicted and very important effect has been observed in some of the parabolic flight test data but can be confirmed only by upcoming long-term zero-gravity experiments in orbit.

Quantitative Examples of the Coupled Fluid-Spacecraft Response

The general trends and conclusions discussed above are illustrated here by specific experimental data and analytical predictions. Again, impulsive free decay data are presented and discussed before the resonance data.

Figures 4 and 5 show typical experimental nonlinear free decay measurement of the spacecraft degree of freedom $x(t)$ for the system ($Bo = 66$, $\mu = 0.15$, $\nu = 1.07$, photoflo). In Fig. 4, the response to three values of Ξ_{ex}(0.062, 0.043, and 0.013) have been normalized by Ξ_{ex} and overplotted. The initial conditions, $x(0)/d$, are proportional to the Ξ_{ex}, so the normalized measurements overlay at $t = 0$. For $t > 0$, however, the responses $x(t)$ do not overlay. The nonlinear effects of the slosh change the natural period of oscillation in the response. The fact that the phase in the response to a larger impulse lags the response at a smaller impulse confirms the analytical prediction (for this system) that the natural frequencies of the coupled system decrease with increasing modal amplitude.

To measure the frequency shift during the free decay, the linear identification algorithm, ERA (eigensystem realization algorithm),[29] was applied to incremental windows of data. The ERA data windows were four to five oscillation periods long, while the increment between windows was very small. The identified modal frequencies represented *average* natural vibration frequencies during the data window. Because the average amplitude decreases during successive ERA data windows, the ERA-averaged modal frequency measurements changed to reflect the effect of the nonlinearity on the vibration frequencies. The nonlinear frequency shift due to amplitude of the coupled motion was consistently measured by this method, and qualitative trends could be identified.

Figure 5 presents the windowed ERA identification of the largest initial condition free decay presented in Fig. 4. The nonlinear theory predicted by the planar analytical model is also plotted. The extent of the nonlinear frequency shift is averaged by the ERA data window, and therefore the ERA identified eigenfrequency shift is consistently less than that predicted by the analytical model.

Figure 6 presents the windowed ERA experimental results and the analytical predictions for the same system ($\mu = 0.16$, $\nu = 1.09$) at each of the four Bond numbers studied and for an initial impulse $\Xi_{ex} = 0.043$. The response at $Bo = 33$ is partic-

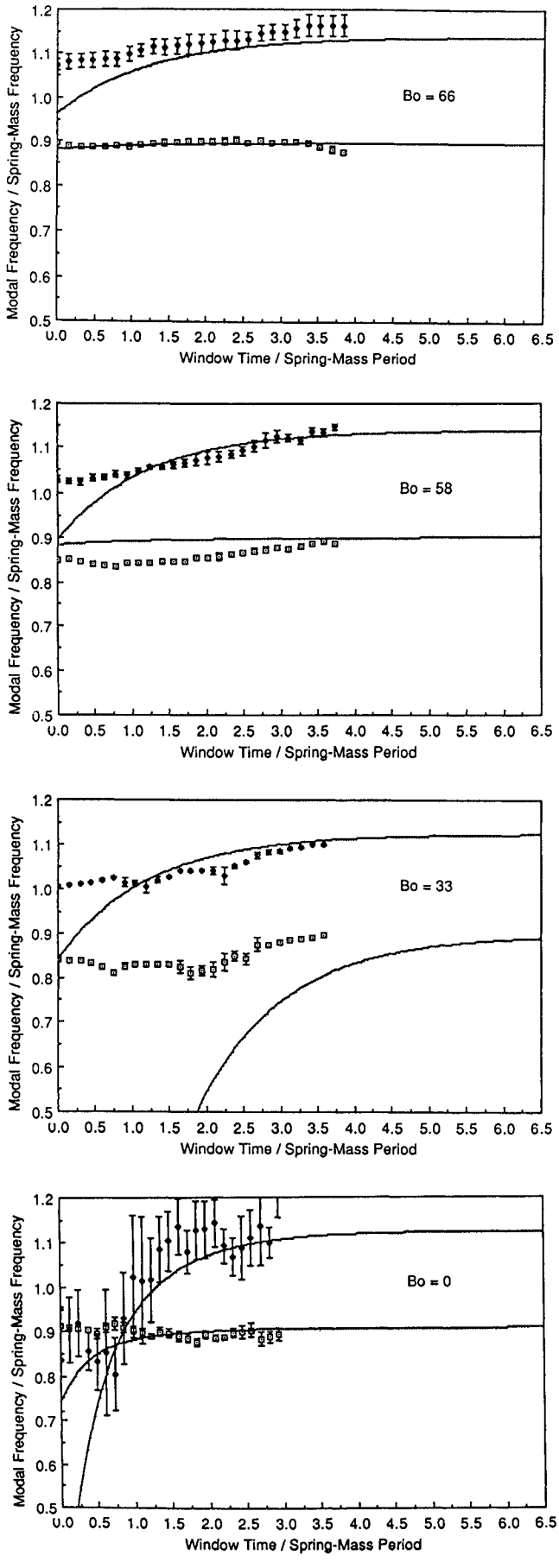

Fig. 6 Windowed ERA results and analytical predictions for the system ($\mu = 0.16$, $v = 1.09$) at each of the four Bond numbers studied and for $\Xi_{ex} = 0.43$ ($Bo = 0$ results are parabolic flight test 0 g experimental data).

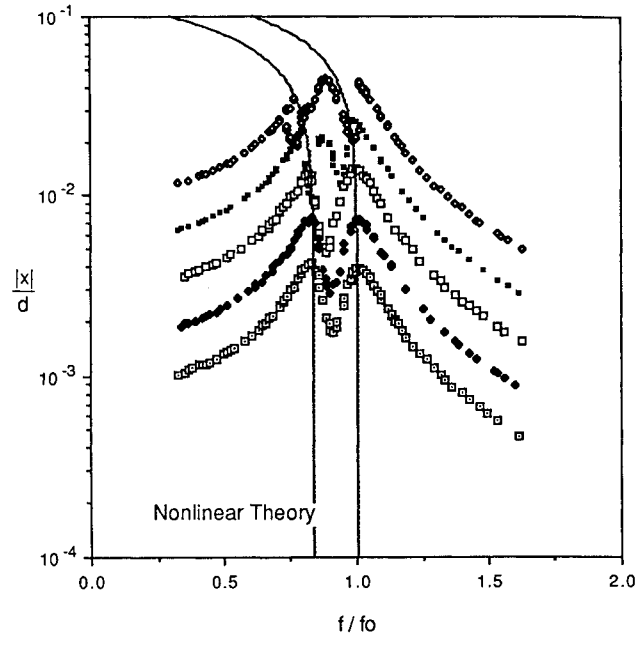

Fig. 7 Resonance of the spacecraft degree of freedom x for the system ($Bo = 66$, $\mu = 0.16$, $v = 0.90$, photoflo) at $|\Xi_{ex}| = 0.0010$, 0.0018, 0.0032, 0.0056, and 0.0100. Theoretical position of the resonance peaks for planar motion are also plotted.

ularly interesting. The analysis predicts very large nonlinear frequency shifts at this Bo due to the resonance between the first fluid-spacecraft eigenmode and one secondary fluid mode. Under this condition, the analytical model should treat the secondary fluid mode as the same order as the primary fluid mode. The saturation phenomenon observed experimentally for this system was observed for all the experimental systems that were close to a particular internal resonance.

The coupled harmonic resonance data reflect many of the same trends observed in the impulse response data. Figure 7 overplots the amplitude of the spacecraft response x/d against excitation frequency $\omega/\sqrt{k/m}$ for each of the five values of $|\Xi_{ex}|$ applied. The range of harmonic resonance amplitudes studied experimentally ($0.001 < |\Xi_{ex}| < 0.010$) extended from an apparently linear response ($|\Xi_{ex}| < 0.002$), through a region for which the nonlinear, restricted planar analysis applied ($0.002 < |\Xi_{ex}| < 0.006$), and into a region of large nonplanar, multivalued nonlinearity ($|\Xi_{ex}| > 0.006$). The nonlinear backbone curves from the planar nonlinear analysis for each of the two fluid-spacecraft eigenmodes are also plotted. The analytical prediction follows the location of the resonance peaks up to the onset of the nonplanar motion. For this particular coupled system ($Bo = 66$, $\mu = 0.16$, $v = 0.90$, photoflo), nonplanar fluid motion occurred at each of the two higher-amplitude plots.

Figure 8 plots the amplitudes and the phases of the spacecraft response x and each of the measured reaction slosh forces F_{xs} (planar) and F_{ys} (nonplanar) at the largest of these resonances. The resonance diagram at this excitation amplitude is very complex: five distinct types of fluid-spacecraft motion were identified for this system. A sixth type was observed in several other systems. Note that this contrasts with the motion of the fluid alone, which exhibits only three types of nonlinear motion.

The six types of resonance motions observed in the coupled system are distinguished by the motion of the free surface vibration node line, as diagrammed in Fig. 9. Type 1, planar I motion, is identical to the ordinary planar motion observed in the nonlinear uncoupled slosh resonance. The node line remains stationary but perpendicular to the direction of tank motion. At excitation frequencies above the planar I region, planar II develops. This motion is identical to planar I, except that it is much larger ($\eta \approx a$). The jump to this motion is

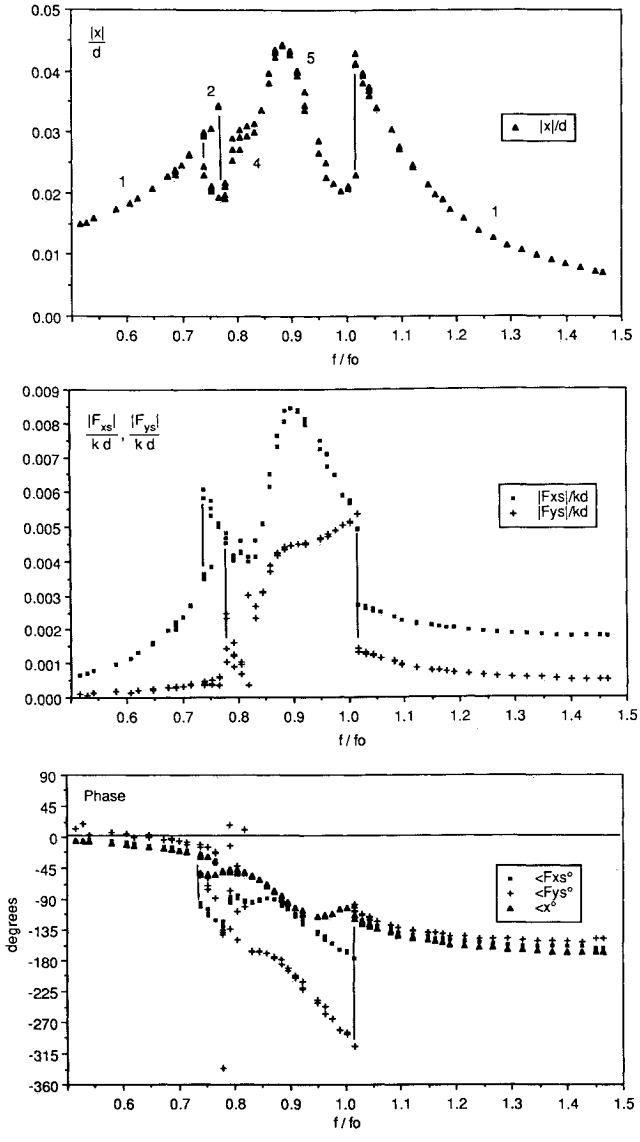

Fig. 8 Resonance response of the system ($Bo = 66$, $\mu = 0.16$, $v = 0.90$, photoflo) at $|\Xi_{ex}| = 0.010$.

distinct and involves the spacecraft motion x as well as the fluid motion. Planar II is unique in the coupled response. Type 3, skew nonplanar motion, is also unique in the coupled system response. In this motion, which occurs just above planar II, the node line is stationary but not perpendicular to the direction of the tank. The force measurements F_{xs} and F_{ys} are both nonzero and are approximately in-phase. Above the skew nonplanar region, PMNR develops just as in the uncoupled fluid resonance. Above PMNR, HNR also develops. It is important to realize that, although PMNR and HNR are similar in the fluid motion as in the uncoupled resonance, the spacecraft motion x also is periodically modulated in PMNR and experiences the same jump phenomena as the fluid in HNR. The sixth type of motion is unique to the coupled system. This motion, designated APMNR for asymmetric PMNR, is an unsymmetric motion of the free surface that has no simple node line. The motion is multiply harmonic, just as in PMNR, and undoubtably is a unique product of the coupled interaction of the fluid and spacecraft motions. APMNR was not observed in the system presented in Fig. 8 but was observed for other systems. At frequencies above the APMNR region, the motion of the fluid transitions back to the planar I motion, and the system response is harmonic. These unusual and unexpected resonance motions were observed in all of the 1 g Bond number test conditions.

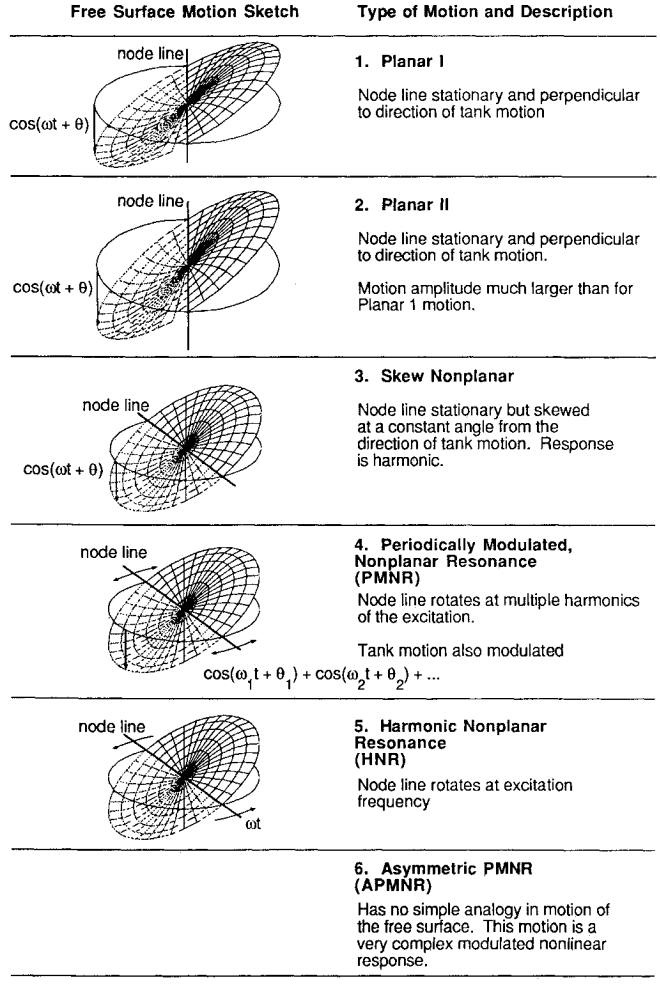

Fig. 9 Types of nonlinear fluid motion observed in the large-amplitude resonance of the coupled systems.

Conclusions

The nonlinear coupled motion of a simple fluid-spacecraft system has been studied both experimentally and analytically. An approximate, analytical fluid-spacecraft model was derived that expressed the fluid motion as a superposition of the linear slosh eigenmodes. The nonlinear kinematic problem for the fluid was solved in an extension of the earlier work of Miles[12] to include a low-gravity equilibrium interface. The coupled Lagrangian was formulated using this approximate kinematic description. Nonlinear capillary forces were included through the nonlinear potential energy of the free surface, in a method similar to that of Limarchenko.[18] For the first time, vibratory motion of the spacecraft was included in the coupled system Lagrangian. In addition, the coupled system equations of motion were found and approximately solved for the special case of restricted planar motion of the fluid.

The experiment systematically studied the parametric dependence of the nonlinear coupled fluid-spacecraft system dynamics. A unique experimental device was developed in which a subscale model tank was coupled to the motion of a simulated, linear spacecraft mode. Both planar and nonplanar reaction slosh forces were measured. The effects of system mass ratio, frequency ratio, and Bond number were all studied both in 1 and 0 g during parabolic flight tests on the NASA KC-135 Reduced Gravity Test Facility.

The results of this research have important implications for the modeling of more complicated systems. It should not be assumed that a linear model of the fluid or even a nonlinear uncoupled model of the fluid will lead to an accurate analytical model if the fluid slosh and spacecraft motions are closely coupled. Higher fluid modes are central to the nonlinear

coupled fluid-spacecraft motion and must always be retained. This means a nonlinear uncoupled pendulum model of the slosh will misrepresent the slosh motion if coupled to a spacecraft model. Furthermore, capillarity should be included for Bond numbers as high as 60–100 because of its effect on the natural frequency of the higher fluid modes. The natural frequency and the type of resonance response of the coupled nonlinear motion will depend on the amplitude of the coupled motion in a way that can be predicted only by a nonlinear coupled model.

The results of this research also have direct application in the design of spacecraft attitude control systems. In particular, a small *nonlinear* difference in the fluid-spacecraft response could be interpreted as an uncertainty in the *linear* control system design model. If, for instance, the nonlinear model predicted an eigenfrequency shift of 10% over the expected range of disturbances, then the attitude control system should be designed to tolerate such an uncertainty in the plant model. Of course, if the model predicted that the fluid-spacecraft motion bifurcates, leading, for instance, to transverse fluid motion, then the stability and performance of the linear control algorithm would be in serious doubt.

Acknowledgments

This paper reports on research performed at the Massachusetts Institute of Technology. It was sponsored by the Boeing Aerospace Company, with Dr. Jere Meserole as technical monitor, and by NASA Headquarters Grant NAGW-21, with Mr. Samuel Venneri as technical monitor. Dr. R. E. Shurney of the Marshall Spaceflight Center coordinated and assisted with the NASA KC-135 parabolic flight tests of the experimental phase of this research. The preparation of this document was sponsored in part at Sandia National Laboratories under U.S. Department of Energy Contract DE-AC04-76DP00789.

References

[1]Abramson, H. N., *The Dynamic Behavior of Liquids in Moving Containers*, NASA SP-106, 1966.

[2]Wie, B., "Thrust Vector Control Design for a Liquid Upper Stage Spacecraft," *Journal of Guidance, Control and Dynamics*, Vol. 8, Sept.–Oct. 1985, pp. 566–572.

[3]Fester, D. A., Rudolph, L. K., and Kiefel, E. R., "A Space Station Tethered Orbiral Refueling Facility," AIAA Paper 85-1160, July 1985.

[4]Satterlee, H. M. and Reynolds, W. C., "The Dynamics of the Free Liquid Surface in Cylindrical Containers Under Strong Capillary and Weak Gravity Conditions," Stanford Univ., Stanford, CA, TR-LG-2, 1964.

[5]Eide, D. G., "Preliminary Analysis of Variation of Pitch Motion of a Vehicle in a Space Environment Due to Fuel Sloshing in a Rectangular Tank," NASA TN D-2336, 1964.

[6]Yeh, G. C. K., "Free and Forced Oscillations of a Liquid in an Axisymmetric Tank at Low-Gravity Environments," *Journal of Applied Mechanics*, Vol. 34, Ser. E, No. 1, March 1967, pp. 23–28.

[7]Chu, W. H., "Low-Gravity Fuel Sloshing in an Arbitrary Axisymmetric Rigid Tank," *Journal of Applied Mechanics*, Vol. 37, Ser. E, No. 7, Sept. 1970, pp. 828–837.

[8]Wohlen, R. L., Park, A. C., and Warner, D. M., "Finite Element Solution of Low Bond Number Sloshing," Martin-Marietta, Denver, CO, Contractor Rept. MCR-75-139, Contract NAS8-29946, 1975.

[9]Dodge, F. T. and Garza, L. R. "Experimental and Theoretical Studies of Liquid Sloshing at Simulated Low Gravity," *Journal of Applied Mechanics*, Vol. 34, Ser. E, No. 3, 1967, pp. 555–562.

[10]Meserole, J. S. and Fortini, A., "Slosh Dynamics in a Toroidal Tank," AIAA Paper 86-1717, June 1986.

[11]Hutton, R. E., "An Investigation of Resonant, Nonlinear, Nonplanar Free Surface Oscillations of a Fluid," NASA TN D-1870, 1964.

[12]Miles, J. W., "Nonlinear Surface Waves in Closed Basins," *Journal of Fluid Mechanics*, Vol. 75, Pt. 3, 1976, pp. 419-448.

[13]Miles, J. W., "Internally Resonant Surface Waves in a Circular Cylinder," *Journal of Fluid Mechanics*, Vol. 149, Dec. 1984, pp. 1–14.

[14]Miles, J. W., "Resonantly Forced Surface Waves in a Circular Cylinder," *Journal of Fluid Mechanics*, Vol. 149, Dec. 1984, pp. 15–31.

[15]Limarchenko, O. S., "Variational Formulation of the Problem on the Motion of a Tank with Fluid," *Dopovidi Akademii Nauk Ukrains'koi RSR, Ser. A*, No. 10, 1978, pp. 903–907 (in Ukranian).

[16]Limarchenko, O. S., "Direct Method for Solution of Nonlinear Dynamics Problems for a Tank with Fluid," *Dopovidi Akademii Nauk Ukrains'koi RSR, Ser. A*, No. 11, 1978, pp. 999–1002 (in Ukranian).

[17]Limarchenko, O. S., "Variational Method Investigation of Problems of Nonlinear Dynamics of a Reservoir with a Liquid," *Soviet Applied Mechanics*, Vol. 16, No. 1, pp. 74–79, (translated from *Prikladnaya Mekhanika*, Vol. 16, No. 1, 1980, pp. 99–105).

[18]Limarchenko, O. S., "Effect of Capillarity on the Dynamics of a Container Liquid System," *Soviet Applied Mechanics*, Vol. 17, No. 6, pp. 601–604, (translated from *Prikladnaya Mekhanika*, Vol. 17, No. 6, 1981, pp. 124–128).

[19]Limarchenko, O. S., "Direct Method of Solving Problems on the Combined Spatial Motions of a Body Fluid System," *Soviet Applied Mechanics*, Vol. 19, No. 8, pp. 715–721, (translated from *Prikladnaya Mekhanika*, Vol. 19, No. 8, 1983, pp. 77–84).

[20]Limarchenko, O. S., "Application of a Variational Method to the Solution of Nonlinear Problems of the Dynamics of Combined Motions of a Tank with Fluid," *Soviet Applied Mechanics*, Vol. 19, No. 11, pp. 1021–1025, (translated from *Prikladnaya Mekhanika*, Vol. 19, No. 11, 1983, pp. 100–104).

[21]Luke, J. C., "A Variational Principle for a Fluid with a Free Surface," *Journal of Fluid Mechanics*, Vol. 27, No. 2, 1967, pp. 395–397.

[22]Komatsu, K., "Non-Linear Slosh Analysis of Liquid in Tanks with Arbitrary Geometries," *International Journal of Non-Linear Mechanics*, Vol. 22, No. 3, 1987, pp. 193–207.

[23]Ibrahim, R. A. and Barr, A. D. S., "Autoparametric Resonance in a Structure Containing a Liquid, Part I: Two Mode Interaction," *Journal of Sound and Vibration*, Vol. 42, No. 2, 1975, pp. 159–179.

[24]Ibrahim, R. A. and Barr, A. D. S., "Autoparametric Resonance in a Structure Containing a Liquid, Part II: Three Mode Interaction," *Journal of Sound and Vibration*, Vol. 42, No. 2, 1975, pp. 181–200.

[25]Peterson, L. D., "The Nonlinear Coupled Dynamics of Fluids and Spacecraft in Low Gravity," Ph.D. Dissertation, Dept. of Aeronautics and Astronautics, Massachusetts Institute of Technology, Cambridge, MA, SSL Rept. 22-87, 1987.

[26]Peterson, L. D. and Van Schoor, M. C., "Nonlinear Analysis of the Coupled Motion of Fluid Spacecraft Systems," (to be published).

[27]Hastings, L. J. and Rutherford, R. III, "Low Gravity Liquid-Vapor Interface Shapes in Axisymmetric Containers and a Computer Simulation," NASA TM X-53790, 1968.

[28]Nayfeh, A. H. and Mook, D. T., *Nonlinear Oscillations*, Wiley, New York, 1979.

[29]Juang, J. and Pappa, R. S., "An Eigensystem Realization Algorithm for Parameter Identification and Model Reduction," *Journal of Guidance, Control and Dynamics*, Vol. 8, Sept.–Oct. 1985, pp. 620–627.